

Microstructure of Two Overaged Al-Mg-Si-Cu Alloys

Jon Holmestad^{1,2}, Calin D. Marioara³, Sigmund J. Andersen³ and Randi Holmestad¹

¹NTNU, Department of Physics, 7491 Trondheim, Norway

²Hydro Aluminium, Research and Technology Development, Romsdalsvegen 1, 6600 Sunndalsøra, Norway

³SINTEF Materials and Chemistry, 7465 Trondheim, Norway

To investigate differences in precipitation coarsening upon ageing at elevated temperatures, two Al-Mg-Si-Cu alloys, one Mg-rich (A) and one Si-rich (B), with similar amount of solutes were studied by Transmission Electron Microscopy during overageing at 250°C. The hardness of alloy A was found to be significantly higher than for alloy B, by producing a fine precipitate microstructure. The fine particles in alloy A consisted of laths/plates extending along $\langle 001 \rangle_{Al}$, having cross-sections along $\langle 100 \rangle_{Al}$ directions. The laths and plates were identified as (disordered) L-phase and C-phase respectively, both which are common precipitates in the Al-Mg-Si-Cu system. Minor transformation to the equilibrium phase Q/Q' was observed. In contrast, alloy B developed a considerably coarser precipitate microstructure; The main phase being Q/Q' laths extending along $\langle 001 \rangle_{Al}$, but with cross-sections oriented along $\langle 510 \rangle_{Al}$. After 100h at 250°C the average cross-section area of precipitates in alloy B was more than three times that of precipitates of alloy A, lengths almost twice as long, while the precipitate number density was about one third. However, both alloys tend towards comparable volume fractions, at levels suggesting that the precipitates consume most solute in both alloys.

Keywords: *6xxx-alloys, Microstructure, Mechanical properties.*

1. Introduction

As a consequence of their superior properties such as high strength to weight ratio, good ductility and corrosion properties, Al-Mg-Si-(Cu) alloys are important industrial materials. The main application has been as extruded profiles, both in the construction industry and increasingly in the automotive industry. The Al-Mg-Si-(Cu) alloys are age-hardening materials, achieving high strength due to the formation of nanometer-sized metastable precipitates in the Al matrix. The metastable precipitates in this system have needle/lath/rod/plate morphologies, with longest direction oriented along $\langle 001 \rangle_{Al}$. Depending on the heat treatment and alloy composition, metastable precipitates with various crystal structures form with different sizes, densities and volume fractions. This has a direct impact on mechanical properties.

The precipitation sequence for the Al-Mg-Si system was found to be [1-5]:

SSSS \rightarrow atomic clusters \rightarrow GP-zones \rightarrow β'' \rightarrow β' , U1, U2, B' \rightarrow β /Si, equilibrium, where SSSS stands for Super Saturated Solid Solution. The U1, U2 and B' phases are also known as Type A, Type B and Type C respectively [2]. It has been demonstrated that GP-zones and β'' are the main hardening phases [1, 4] and the overall hardness decreases upon overageing [5]. The types of precipitates formed upon overageing are controlled by the alloy composition, with different phases having different hardness influence [5]. It was found that U2 formed a finer microstructure with higher hardness than β' and U1 when the alloys had a total solute amount of 1.3 at%, with Mg/Si ratios varying from 1.25 to 0.5.

When Cu is added to Al-Mg-Si alloys, the overall hardness increases and the precipitation sequence changes to [2, 6-9]: SSSS \rightarrow atomic clusters \rightarrow GP zones \rightarrow β'' , L, S, QC \rightarrow Q' \rightarrow Q, equilibrium.

In this system, the amount of β'' is decreasing and a multitude of partly disordered Cu-containing Q' -precursors are responsible for the hardness effect [9]. It was found that Q' phase was produced regardless of Mg/Si ratio in alloys containing 1.3 at% Mg + Si and 0.13 at% Cu. This phase produced higher hardness and finer microstructures compared to similar Cu-free alloys where the microstructure consisted of β' and U2.

In light of the above considerations, the main goal of the present work is to further investigate the effect of overageing on Al-Mg-Si-Cu alloys. In particular, the existence of other precipitates than Q' in the overageing conditions of this system and their connection to hardness was investigated.

2. Experimental procedures

Two Al-Mg-Si-Cu alloys, one Mg-rich (alloy A) and one Si-rich (alloy B) were cast, homogenized 5 hours at 550°C and extruded into 20 mm diameter round profiles. The bars were cut into 120 mm long cylinders, solution heat treated for 30 minutes at 530°C, water quenched, stored 4 hours at room temperature, aged 12 hours at 155°C and water quenched. This resulting T6 condition was then heat treated at 250°C in a sand bath for 100 hours with periodical removal, water-quenching and hardness measurements. The hardness measurements were performed with an Akashi hardness tester. Five indentations were made at each end of the cylinder each time. The load used was 5 kg, the indentation time 15 sec and the load speed was 100 $\mu\text{m}/\text{sec}$. The surface was polished between every second hardness test with SiC polishing paper with fineness up to 1200 grains/ cm^2 .

TEM specimens were selected from the end of the aging procedure, i.e. after 100 h at 250°C. The cylinders were cut into thin slices of ~ 1 mm before grinding with successively finer SiC polishing papers up to 4000 grains/ cm^2 until a thickness of approximately 10 μm was obtained. Small disks were stamped out of this thin foil before they were electropolished with an electrolyte containing 1/3 nitric acid (HNO_3) and 2/3 methanol (CH_3OH). The electrolyte was kept at temperatures between -20°C and -30°C

All images for quantification of precipitate microstructure were taken in bright field mode with a Philips CM30 Transmission Electron Microscope (TEM) operated at 150 kV. Thickness measurements of the imaged areas were performed with a Gatan parallel electron energy loss spectrometer (EELS). Different phases present in the alloys were determined from High Resolution TEM (HRTEM) images recorded with a JEOL 2010F microscope having 0.2 nm point resolution. All images presented in this work were recorded from specimens with the Al-matrix oriented in a $\langle 001 \rangle_{\text{Al}}$ zone axis.

3. Results and discussion

Fig. 1 shows the hardness evolution during overageing of alloy A and B. Both alloys have a similar T6 starting point and achieve a maximum hardness slightly below 120 Vickers. After ageing at 250°C for 15 minutes, the hardness starts to decrease. It can clearly be observed that the resistance to overageing is larger for alloy A than for alloy B.

The microstructure of alloys A and B at the end of overageing (after 100h at 250°C) is shown in Fig. 2 and Fig. 3 respectively. Alloy A produces a finer microstructure as compared to alloy B. Fig. 2 shows that the precipitates in alloy A can be classified in two categories: 1) with more plate-like cross-sections that are oriented along $\langle 100 \rangle_{\text{Al}}$ directions; 2) lath-shaped, having cross-sections oriented along $\langle 510 \rangle_{\text{Al}}$ directions. The particles in category 1 are more numerous than those in category 2. In contrast, Fig. 3 shows that most of the coarse precipitates in alloy B are category 2. The needles in alloy B are much longer and have larger cross-sections than in alloy A. A coarser dislocation network is observable in this alloy as well.

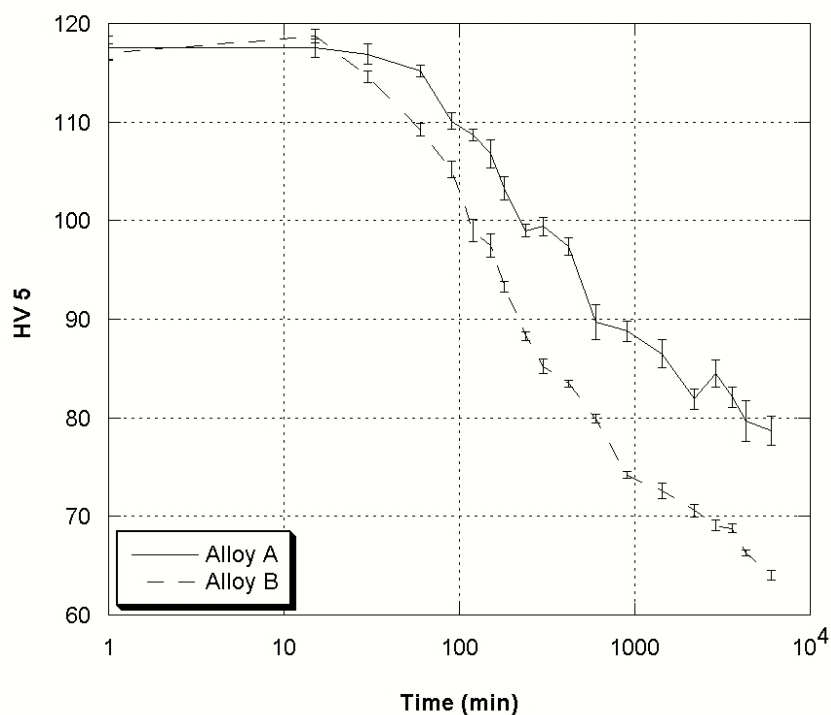


Fig. 1: Hardness evolution at 250°C of the alloys as a function of ageing time up to 100 h from a T6 condition.

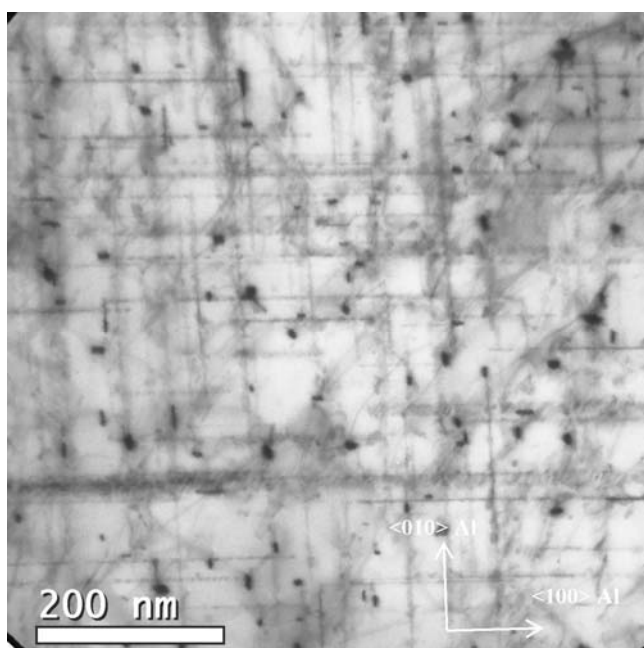


Fig. 2: Bright field TEM image of alloy A after overageing for 100 h at 250°C. Most precipitates have cross-sections oriented along $\langle 100 \rangle$ Al directions.

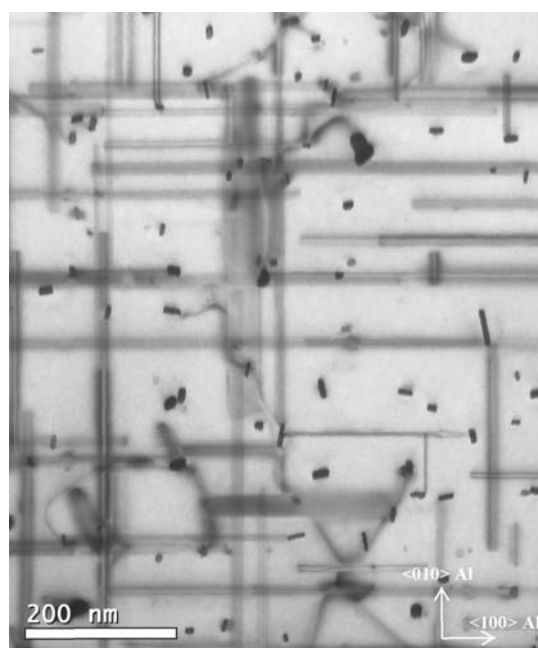


Fig. 3: Bright field TEM image of alloy B after overageing for 100 h at 250°C. Most precipitates have cross-sections oriented along $\langle 510 \rangle$ Al directions

In Table 1, the volume fraction, number density, average needle length and average cross-section of the precipitates in both alloys is presented. The numbers confirm the qualitative differences observed in the bright field images; the precipitate number density is almost three times higher in

alloy A than in alloy B. The precipitate size is larger in alloy B than in alloy A, with an average needle length almost twice as large and an average cross-section almost four times that of alloy A.

Table 1: The volume fraction, number density, average needle length and cross-section of the precipitates in the alloys after ageing.

Alloy	Volume fraction (%)	Number density (μm^{-3})	Average needle length (nm)	Average cross-section (nm^2)
A	1.97+0.237	1024.4+44.1	355.4+9.0	65.2+8.3
B	3.07+0.428	311.3+30.2	673.1+19.9	211.5+28.41

The finer microstructure is likely to be the reason for the higher strength of alloy A: A higher number density of precipitates decreases the average distance between precipitates. This shorter distance makes dislocation motion harder.

Typical HRTEM images of precipitate types 1 and 2 found in alloy A is shown in Fig. 4 and Fig. 5 respectively. It can be seen that type 1 is a L-precipitate [9-10]. When fully ordered, this type of precipitate is a plate called the C-phase, with a monoclinic unit cell having dimensions $a = 1.04 \text{ nm}$, $b = 0.81 \text{ nm}$, $c = 0.405 \text{ nm}$, $\gamma = 101^\circ$ [9-10]. In Fig. 4, one such unit cell is superimposed on the precipitate. The lath-shaped precipitate (Type 2) in Fig. 5 can be classified as a disordered Q'-phase. The Q' phase has a hexagonal unit cell with dimensions $a = b = 1.04 \text{ nm}$, $c = 0.405 \text{ nm}$ [11]. One Q' unit cell is superimposed on the precipitate shown in Fig. 5.

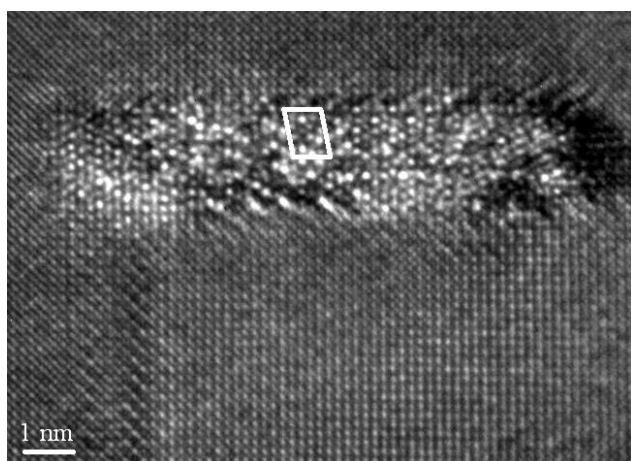


Fig. 4: A HRTEM image of a partially disordered C-type plate precipitate in alloy A. A schematic unit cell is superimposed on part of the ordered structure.

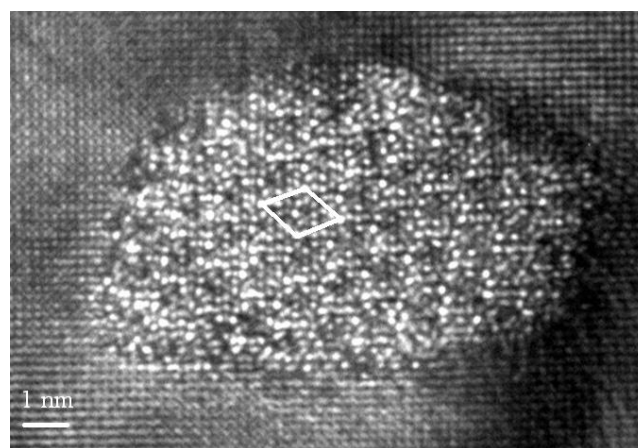


Fig. 5: A HRTEM image of a partially disordered lath-shaped Q'-precipitate in alloy A. A schematic unit cell is superimposed.

In alloy B, HRTEM images show that the precipitates are either disordered (Fig. 6) or perfect Q' precipitates (Fig. 7). As shown earlier, these precipitates are significantly larger than the L-precipitates found in alloy A.

In alloy B, no L-precipitates were observed. It is likely this phase also forms in this alloy, but have transformed to Q', which indicates that the precipitation kinetics is faster in alloy B than in alloy A. Further experiments are required to determine this.

These results indicate that the high strength of alloy A during overageing is caused by the formation of a fine microstructure of L-precipitates. As the L-precipitates are precursors of Q' phase, with structural similarities between the two phases, the difference in microstructure seems to arise from the different connection of precipitate cross-section plane with the Al matrix; along $\langle 100 \rangle$ Al in the case of L-precipitates and along $\langle 510 \rangle$ in the case of Q'. The L-phase also shows a high stability

during overageing, with only few precipitates transforming into Q' even after 100h at 250°C. In alloy A, some precipitates were observed showing both C-plate and Q' unit cells.

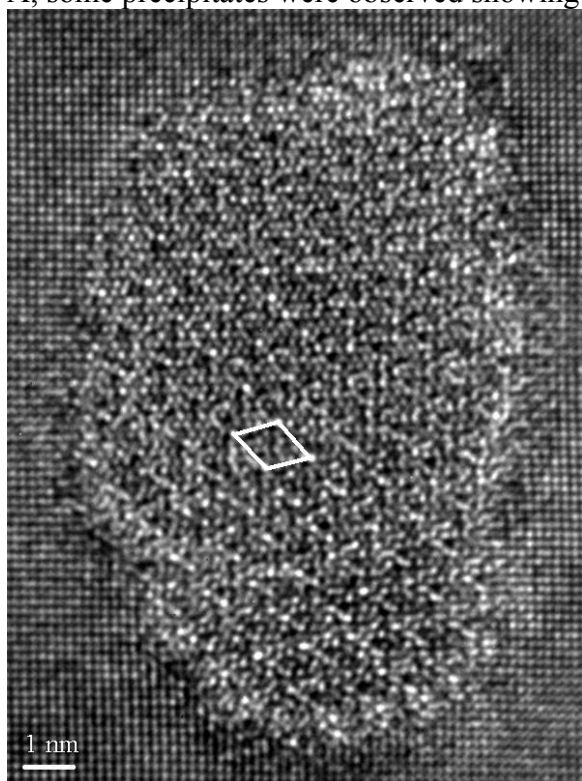


Fig. 6: A HRTEM image of a partially disordered Q'-precipitate in alloy B. A schematic unit cell is superimposed.

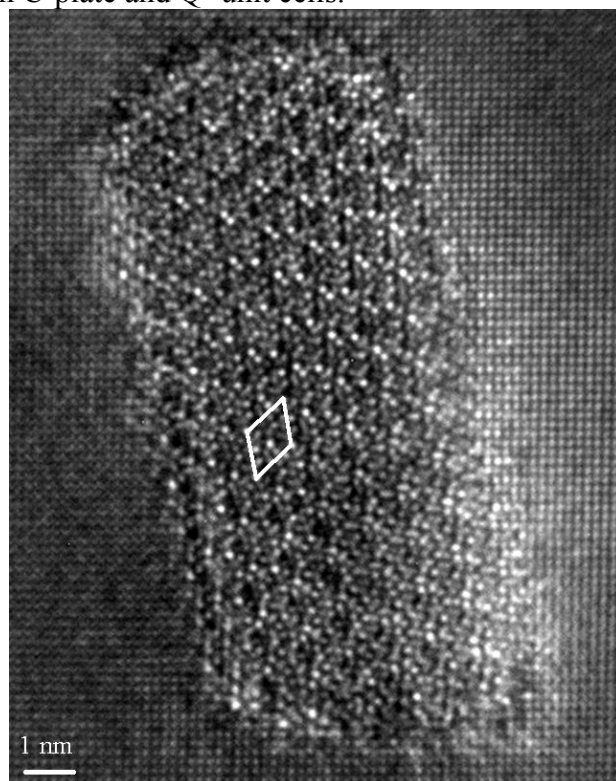


Fig. 7: A HRTEM image of a perfect Q'-precipitate in alloy B. A schematic unit cell is superimposed

4. Conclusion

During overageing, the Mg-rich alloy A shows significantly higher hardness than the Si-rich alloy B. The higher hardness in alloy A is caused by a fine microstructure of L-precipitates, while in alloy B mainly Q' precipitates were observed. The volume fractions after 100h overageing at 250°C indicate that most of the solutes have been used for precipitate formation.

5. Acknowledgments

This work was financially supported by *The Research Council of Norway* via the BIA project 'Kimdanningskontroll (Nucleation Control)', which is supported by the industry; Hydro Aluminium AS, Steertec Raufoss AS.

References

1. Edwards, G.A., et al., *The precipitation sequence in Al-Mg-Si alloys*. *Acta Materialia*, 1998. **46**(11): p. 3893-3904.
2. Matsuda, K., et al., *Precipitation sequence of various kinds of metastable phases in Al-1.0mass% Mg2Si-0.4mass% Si alloy*. *Journal of Materials Science*, 2000. **35**(1): p. 179-189.
3. Matsuda, K., et al., *Metastable phases in an Al-Mg-Si alloy containing copper*. *Metallurgical and Materials Transactions A*, 2001. **32**(6): p. 1293-1299.

4. Marioara, C.D., et al., *The influence of alloy composition on precipitates of the Al-Mg-Si system*. Metallurgical and Materials Transactions A, 2005. **36**(3): p. 691-702.
5. Marioara, C.D., et al., *Post- β'' phases and their influence on microstructure and hardness in 6xxx Al-Mg-Si alloys*. Journal of Materials Science, 2006. **41**(2): p. 471-478.
6. Cayron, C., et al., *Structural phase transition in Al-Cu-Mg-Si alloys by transmission electron microscopy study on an Al-4wt% Cu-1 wt% Mg-Ag alloy reinforced by SiC particles*. Philosophical Magazine A, 1999. **79**(11): p. 2833-2851.
7. Miao, W.F. and D.E. Laughlin, *Effects of Cu content and preaging on precipitation characteristics in aluminum alloy 6022*. Metallurgical and Materials Transactions A, 2000. **31**(2): p. 361-371.
8. Chakrabarti, D.J. and D.E. Laughlin, *Phase relations and precipitation in Al-Mg-Si alloys with Cu additions*. Progress in Materials Science, 2004. **49**(3-4): p. 389-410.
9. Marioara, C.D., et al., *The effect of Cu on precipitation in Al-Mg-Si alloys*. Philosophical Magazine A, 2007. **87**(23): p. 3385-3413.
10. Torsæter, M., et al., *Crystal Structure Determination of the Q' and C-type Plate Precipitates in Al-Mg-Si-Cu (6xxx) Alloys*, in *ICAA11*. 2008: Aachen.
11. Ravi, C. and C. Wolverton, *First-principles study of crystal structure and stability of Al-Mg-Si-(Cu) precipitates*. Acta Materialia, 2004. **52**: p. 4213-4227.